CHEMMEDCHEM

CHEMISTRY ENABLING DRUG DISCOVERY

Accepted Article

Title: Ectonucleotidase inhibitory and redox activity of imidazole-based organic salts and ionic liquids

Authors: Fliur Macaev, Veaceslav Boldescu, Natalia Sucman, Sidra Hassan, Jamshed Iqbal, Mariana Neam□u, Joanna Lecka, Jean Sevigny, and Denis Prodius

To be cited as: *ChemMedChem* 10.1002/cmdc.201800520

Link to VoR: http://dx.doi.org/10.1002/cmdc.201800520

A Journal of

ChemPubSoc Europe

WILEY-VCH

www.chemmedchem.org

Ectonucleotidase inhibitory and redox activity of imidazole-based organic salts and ionic liquids

Veaceslav Boldescu,[a] Natalia Sucman,[a] Sidra Hassan,[b] Jamshed Iqbal,[b] Mariana Neamtu,[c] Joanna Lecka,[d] Jean Sévigny,[d] Denis Prodius,[e] and Fliur Macaev*[a]

[a] Dr. Veaceslav Boldescu, Dr. Natalia Sucman, Prof. Fliur Macaev
Laboratory of Organic Synthesis and Biopharmaceuticals
Institute of Chemistry
3 Academiei str., 2028 Chisinau, Moldova
E-mail: flmacaev@cc.acad.md
[b] Dr. Jamshed Iqbal, Sidra Hasan
Department of Pharmaceutical Sciences
COMSATS Institute of Information Technology
22060 Abbottabad, Pakistan
[c] Dr. Mariana Neamtu
Interdisciplinary Research Department
„Alexandru Ioan Cuza" University
54 Lascar Catargi str., 700107 Iasi, Romania
[d] Joanna Lecka, Dr. Jean Sévigny
Département de microbiologie-infectiologie et d'immunologie,
Faculté de Médecine, Université Laval, Québec, QC, G1V 0A6, Canada
Centre de Recherche du CHU de Québec – Université Laval, Québec, QC, G1V 4G2, Canada
[e] Dr. Denis Prodius
Laboratory of Bioinorganic Chemistry and Nanocomposites
Institute of Chemistry
3 Academiei str., 2028 Chisinau, Moldova
Current address: Ames Laboratory
U.S. Department of Energy and Critical Materials Institute
Ames, Iowa, 50011-3020, USA

Supporting information for this article is given via a link at the end of the document.

Abstract: Cytotoxicity against cancerous and normal cells, inhibition of ectonucleotidase, and redox properties of a new group of imidazole-based organic salts and ionic liquids have been studied. The tetrachloroferrate salt of a 1-methylimidazole derivative of salicylic aldehyde has been shown to have most prominent inhibitory activity against ectonucleotidase, as well as a higher cytotoxicity against HeLa cells than that of the reference compound carboplatin, while having lower cytotoxicity towards BHK-21 cells. The studied compounds have shown a moderate level of antioxidant activity with better results for the salicylic aldehyde derivatives than for the spiropyrans. Moreover, the compounds did not generate singlet oxygen formation.

Introduction

The multifunctionality including the anticancer potential of organic salts and ionic liquids (OSILs) has been widely discussed recently.[1-11] Their attractiveness for pharmaceutical production is attributed to such advantageous properties as simplicity in preparation and purification, low costs, tunable permeability through biological barriers, etc.[12]

Most of the previous studies by other groups[13–17] on OSILs with more or less selective cytotoxicity against different lines of cancerous cells have mainly demonstrated the antiproliferative activity. Other works made attempts for structure-cytotoxic activity relationship studies that demonstrated higher toxicity for OSILs containing cations with longer chains and lower toxicity for compounds with functionalized side chains in cations as compared to non-functionalized ones.[14,18,19] Wang et al.[20] studied cytotoxicity of a group of ionic liquids and their precursors in HeLa cells and determined increase in reactive oxygen species production (ROS) and a consequent reduction of mitochondrial membrane potential. At the same time, photoinduced electron transfer has been demonstrated for 2,4,6-triphenylthiapyrylium in ionic liquid bmim-PF_6.[21] This study has demonstrated that a highly polar medium formed by ionic liquid stabilizes the formed organic intermediates, thus increasing their live span. A thorough review of the biological effects of OSILs and particularly of their anticancer effect has detected three main mechanisms of their antiproliferative activity: oxidative stress, DNA damage and induction of apoptosis in cells.[22,23] Anticarcinogenic properties of anthocyanidins are attributed to their property to scavenge different mutagenic types of free radicals like reactive oxygen and nitrogen species(ROS/RNS).[24] At the same time, despite their antioxidative nature, anthocyanidins have been found to selectively induce a strong prooxidative and proapoptotic effect in tumour cells.[25] While it is well known that intracellular generation of singlet oxygen equally induces cell death in both cancerous and noncancerous cells, extracellular singlet oxygen has a more selective action on tumour cells via membrane-associated catalase inhibition and reactivation of intracellular ROS/RNS-dependent apoptosis-inducing signalling, while having no effect on non-malignant cells.[26]

Here, we report a group of imidazole-based OSILs **1 – 8** (Figure 1) with cytotoxic activity comparable with that of carboplatin against cancerous cells and much lower against noncancerous cells. Biological tests of the obtained compounds have demonstrated that they possess inhibitory activity against two ectonucleotidase isozymes and this could be one of their main

antiproliferation mechanisms of action. The results of the exploration of the singlet oxygen formation and antioxidant activity of the studied compounds are also presented.

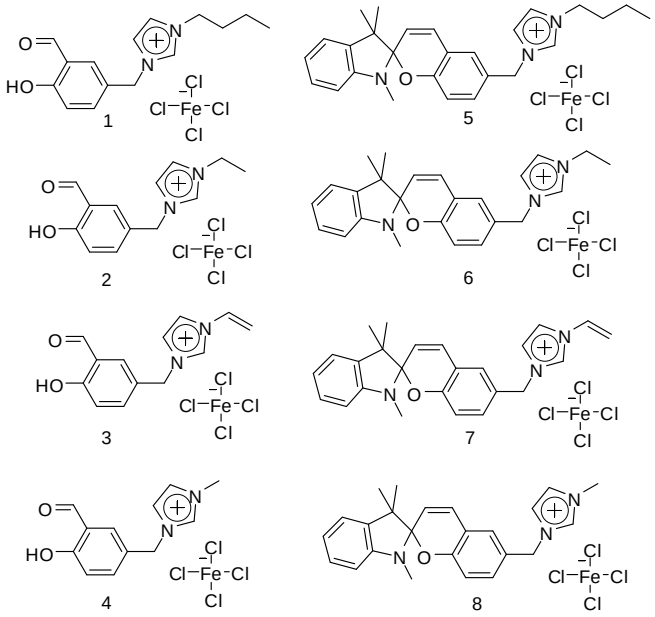

Figure 1. Imidazole-based OSILs **1-8.**

Results and Discussion

Chemistry

The synthesis of the compounds **1-8** has been performed according to the Scheme 1.

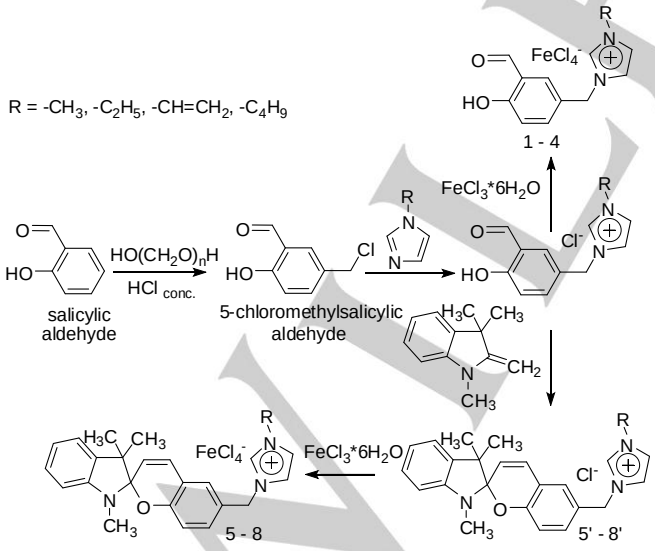

Scheme 1. Synthesis of imidazole-based OSILs **1-8.**

A detailed description of each step is offered in the Experimental section. The FT-IR spectra of the obtained tetracholoroferrates **5-8** include an approximate stretching ranging from 3200 to 2800 cm^{-1} corresponding to the C-H stretching vibration. At the same time, the C-O-C stretching vibration observed at 1262 cm^{-1} and 1076 cm^{-1}. Moreover, the C-O_{spiro} stretching frequencies were noticed at 983 cm^{-1} - 906 cm^{-1} that point to the indolinobenzospiropyran structure. The C=O bond vibration that appears only in open state of spiropyrans is not appearing in the IR spectra of **5-8** in the region 1720-1725 cm^{-1}.

*X-ray investigation of crystal structure (**4**)*

The X-ray measurements for **4** were carried out on a Stoe IPDS II area detector diffractometer at room temperature, using graphite monochromated Mo-Kα radiation (0.7107 Å). Compound **4** crystallizes in the monoclinic $P2_1/n$ space group (*see* Experimental Section/Chemistry) and its asymmetric unit contains a $[FeCl_4]^-$ unit and one protonated ligand molecule for charge balance purposes (Figure 2).

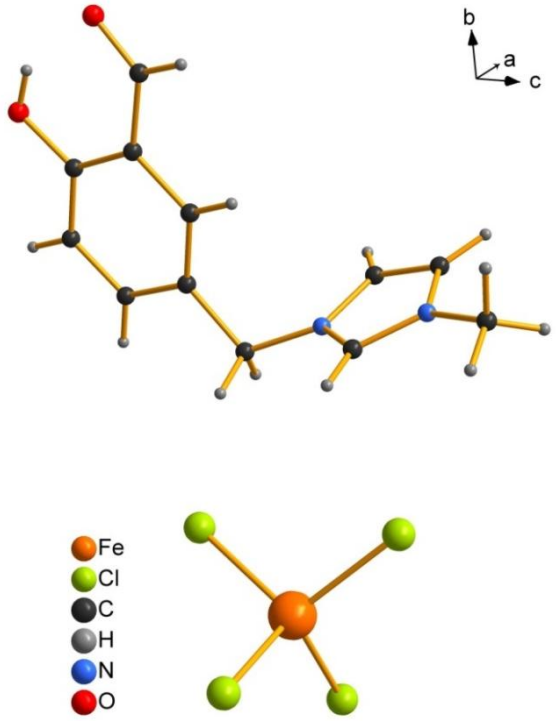

Figure 2. Molecular fragment of compound **4**.

The iron(III) atom is situated in the center of an ideal tetrahedron. The stability of this architecture is further supported by the formation of several weak interactions including C-H···O and C-H···Cl bonds between atoms from two different ligands as well weak π-π interactions between adjacent salicylic units.

Ecto-5'-Nucleotidase Inhibition Studies and SAR

Imidazolium-bearing OSILs **1-8** have been synthesized and tested against two isozymes of ecto-5'-nucleotidase i.e. *h*-e5'NT and *r*-e5'NT. Most of the compounds from both series exhibited maximum inhibitory potential towards both isozymes but few derivatives from either series exhibited selective inhibition towards human isozymes (Table 1). Among all imidazole derivatives compound **4** was found as the potent inhibitor. This compound exhibited non-selective and almost equipotent behaviour towards both isozymes i.e. *h*-e5'NT and *r*-e5'NT with

an IC_{50} value of 1.14±0.05 and 1.93±0.21 μM, respectively. It can be suggested that the substitution of methyl group might be responsible for its maximum inhibition towards both *h*-e5'NT and *r*-e5'NT. Although this compound was found as potent one but the aim of selectivity was achieved in case of **5, 6** and **7** as they exhibited selective inhibition towards *h*-e5'NT with IC_{50} values of 1.36±0.11, 26.1±1.68 and 4.82±0.23 μM, respectively. It was observed from their detailed structure that the increase in carbon number results in the reduced inhibitory activity as observed in case of **6.** The structural activity of **6** and **7** suggested that the presence of unsaturated substituent in **7** results in the 5 folds reduced activity in comparison to **6**. An inverse behaviour was observed in the case of *r*-e5'NT isozyme, derivative **2**, **3**, and **4** exhibited almost equipotent behaviour. It can be suggested from their structure that the presence of instauration is favourable towards inhibition of *r*-e5'NT as seen in case of **2** (1.11±0.05 μM). Compound **3** (1.23±0.01 μM) having ethyl fragment exhibited a little bit higher inhibition as compared to compound **4** (1.93±0.21 μM).

Table 1. Ecto-5'-Nucleotidase (*h*-e5'NT and *r*-e5'NT) inhibition data for the imidazole compounds

Compound	*h*-e5'NT	*r*-e5'NT
	(IC_{50} (μM) ± SEM)[a] / (% inhibition ± SEM)[b]	
1	NT	NT
2	8.14 ± 1.21[a]	1.23 ± 0.01[a]
3	20.2 ± 1.45[a]	1.11 ± 0.05[a]
4	1.14 ± 0.05[b]	1.93 ± 0.21[b]
5	1.36 ± 0.11[a]	32.9 ± 0.45[b]
6	26.1 ± 1.68[a]	12.7 ± 0.18[b]
7	4.82 ± 0.23[a]	15.8 ± 0.11[b]
8	16.1 ± 1.35[a]	18.1 ± 0.98[a]
Sulfamic acid	42.1 ± 7.80[a]	77.3 ± 7.00[a]

[a] The IC_{50} is the concentration of compound at which 50% of the enzyme activity is inhibited. [b] The % inhibition is caused by 100 μM of the tested compounds, NT- not tested

The anticancer potential of the selected derivatives was determined against HeLa cells, in comparison to normal cells i.e., BHK-21 cells. Almost all the compounds exhibited more than 50% inhibition of HeLa cells and among those compounds **2**, **5**, **6**, **7**, and **8** exhibited 68%, 62%, 67%, 64%, and 67% inhibition, respectively. While compound **3** exhibited 73% inhibition. The maximum inhibition was observed in the case of **4**, 87%. The results were in correlation with the enzyme inhibition data. From both series the compounds which were identified as the most potent inhibitor of *h*-e5'NT were also found to inhibit maximum cell growth of HeLa cells. **4** caused maximum inhibition and further selected for the determination of IC_{50} value. It came out with a significant IC_{50} value 2.92±0.11 μM that was approximately 2 fold higher as that of positive control used i.e. carboplatin (5.13±0.45 μM) at the same concentration i.e. 100 μM. These compounds were found safe and did not exhibit ≥10 inhibition of normal cells (Figure 3).

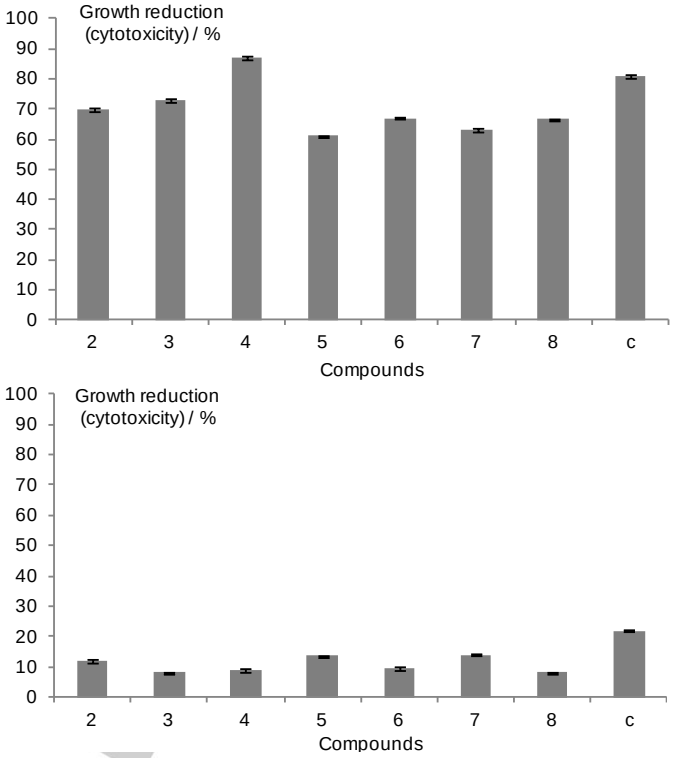

Figure 3. Cytotoxic potential of imidazolium derivatives on HeLa (up) and BHK-21 cells (down). **c –** carboplatin as control. The mean of three experiments ± S.D. is shown.

Cell Cycle Analysis and Apoptosis by Flow Cytometry

Compound **4** induced maximum apoptosis against HeLa cancer cells, i.e. 30.2% as compared to respective positive control i.e. carboplatin (24.5%). The cell cycle analysis of **4** showed that in comparison to the negative and positive control, it intercalated with the DNA molecule of HeLa cells and resulted in significant apoptotic cell death with respect to S phase. Figure 4 represents the percentages of different cell cycle phases such as G_0, G_1, S, and G_2/ M.

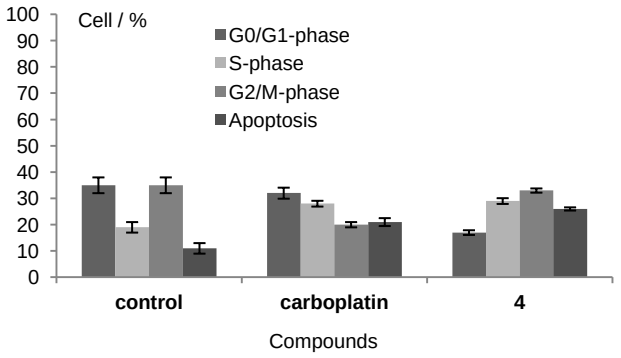

Figure 4. Negative control, carboplatin as positive control and compound **4** induced apoptosis in HeLa cells as demonstrated by flow cytometry analysis employing PI. One way analysis of variance (ANOVA) was used for Data analysis. The mean of three experiments ± S.D. is shown. ***p<0.0001

The activity of compound **4** significantly correlates with the MTT results as it induced significantly higher pro-apoptotic activity as compared to positive control.

Morphological evaluation of Apoptosis

DAPI and PI fluorescent dyes were used to observe DNA condensation which is a major sign of apoptosis (Figure 5). HeLa cells were incubated with the most potent compound **1** (1.14 μM), to examine any sign of apoptosis. The obtained results showed maximum nuclear and chromatin condensation as compared to negative control.

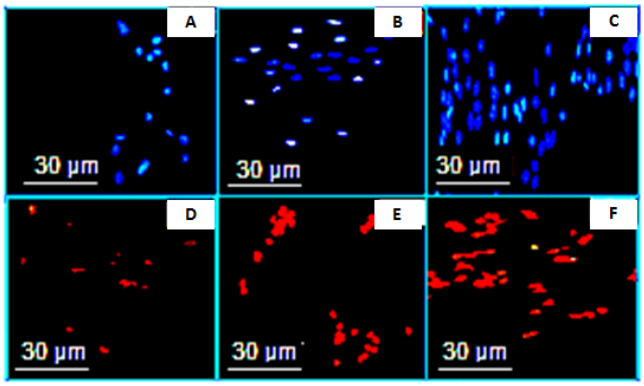

Figure 5. Apoptosis evaluation by fluorescence microscopy: (A) Untreated HeLa cells with DAPI staining; (B) Carboplatin with DAPI staining; (C) **1** with DAPI staining; (D) Untreated HeLa cells with PI staining; (E) Carboplatin with PI staining; (F) **4** with PI staining.

Antioxidant activity of the studied compounds

Antioxidant activity of the **1 – 8** was measured with application of DPPH method and compared to that of the ascorbic acid measured by the same method. In general, compounds **1 – 4** (Figure 6) have shown higher levels of antioxidant activity than compounds **5 – 8** (Figure 7).

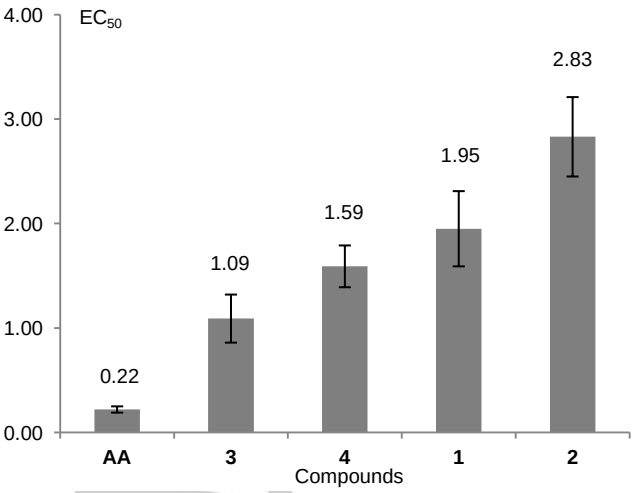

Figure 6. Antioxidant activity of the compounds **1** - **4** expressed in EC_{50}. **AA** – ascorbic acid. The mean of three experiments ± S.D. is shown.

This fact can be explained by the presence of the salicylic aldehyde moiety in the structure of these compounds.

At the same time, there is no clear correlation between the antioxidant activity of the compounds within the groups and their structural particularities. Thus, the main structural difference within both groups is the substituent at the imidazole cycle: methyl, ethyl, vinyl, and butyl. However, there is no clear influence of the substituent nature on the antioxidant activity of the compounds. For example, the highest antioxidant activity represented by lower EC_{50} has been determined for the vinyl derivative **3** in the **1-4** group with salicylic aldehyde moiety and for the methyl derivative **5** in the group **5 – 8.** Moreover, the general trend of the antioxidant activity change in the group of derivatives **1 – 4** in comparison to ascorbic acid (AA) is the following: AA > vinyl > methyl > butyl > ethyl. While the same trend among the **5 – 8** derivatives and ascorbic acid is: AA > butyl > methyl > vinyl > ethyl.

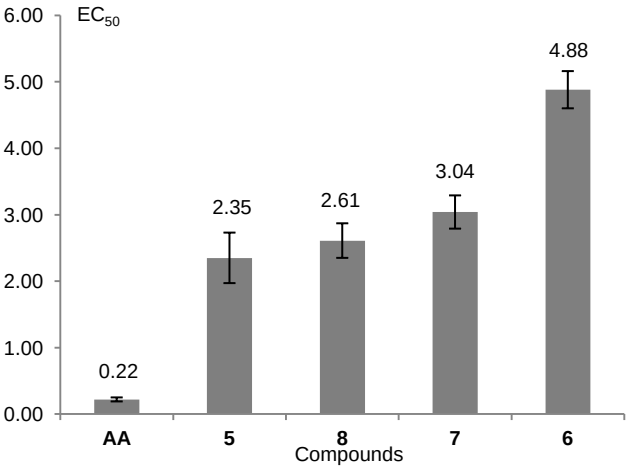

Figure 7. Antioxidant activity of the compounds **5** - **8** expressed in EC_{50}. **AA** – ascorbic acid. The mean of three experiments ± S.D. is shown.

Molecularity trends for each of the groups of the compounds are the following: **3** (0.66) > **1** (0.33) > **4** (0.27) > **2** (0.18) and **8** (0.33) > **5** (0.24) > **7** (0.20) > **6** (0.13). Molecularity represents the number of DPPH molecules that can be reduced by one molecule of the substrate.

Previously, a group of imidazolium-based ionic liquids with antioxidant properties has been reported by Cai et al.[27] The group has reported on antioxidant properties of (BHT-1) $MIMPF_6$ and other imidazolium derivatives detected via rotative bomb oxidation test and thermal analysis. These properties allowed the use of these antioxidants as an anti-wear and antioxidative additive in PEG for steel/steel contacts.

Another group of imidazolium-bearing antioxidative ionic liquids has been reported by Cai et al.[28] These compounds contain 1-(1*H*-benzo[d]p[1,2,3]triazole-1-yl)methyl)-3-methylimidazolium with different anions (PF_6, BF_6, NTf_2) and they can act as low molecular weight gelators. They have been shown to increase resistance to oxygen attack in lubricants at friction. No antioxidant activity parameters have been reported in any of these investigations.

Electron spin resonance investigation

To follow the formation and quenching of the photosensitized singlet molecular oxygen, $^1O_2$, generated by our compounds, the ESR was employed by using 2,2,6,6-tetramethyl-4-piperidinol (TMP-OH) as a spin trap. According to the literature, the diamagnetic scavenger TMP-OH reacts with $^1O_2$, yielding a stable paramagnetic product, 4-hydroxy-2,2,6,6-tetramethylpiperidine-1-oxyl (TEMPOL)[29] that can be easily detected by ESR. Although other ROS can also lead to the formation of TEMPOL,[30] the reactive scavenging of $^1O_2$ by TMP-OH is considered to be highly specific for $^1O_2$.[30] Figure SI1 in Supporting information shows the ESR spectra obtained from the samples containing TMP-OH in the presence of compounds under UVA illumination.

As Figure SI1 shows, no three equidistant and equi-intense hyperfine lines in ESR spectrum, typical for TEMPOL, comparing with control solution (containing only TMP-OH) exposed to UVA illumination for 60 minutes, couldn't observe. This suggests that the compounds don't generate singlet oxygen, even at exposure to different irradiation wavelengths (SI, Figure SI1). For all compounds the presence of an ESR signal near 335 mT could correspond to some organic radicals, probably radical cation SP•+. We can assume, according to the literature, that these compounds were able to change their oxidation state in the presence of iron cations and upon irradiation.[31–34] Upon addition of the iron (III) ions to spiropyran, the SP form does not transform into the MC isomer but converts into radical cation SP•+ whereas Fe^{3+} reduces to Fe^{2+}. Upon UV irradiation and in the presence of the iron (II) ions, SP•+ is reduced to form the open isomer which forms complexes with Fe^{3+}. It is reported that the MC– Fe^{3+} complexes are not reactive or silent to visible light while the addition of 2,2′-bipyridine, which binds ferric cations more effectively, leads to usual photochromic reversibility.[31–34]

We have also investigated the irradiation of compounds in the presence of 4-hydroxy-2,2,6,6-tetramethylpiperidine-1-oxyl (TEMPOL). We could observe a faster decay of TEMPOL in the presence of spiropyrans with irradiation time (SI, Figure SI2), comparing with control solution (containing only TEMPOL) that indicates inhibition of Reactive Oxygen Species such as •OH radicals formed in Fenton reaction. It could be assumed that nitroxides formation under irradiation could prevent generation of •OH radicals from Fenton reactions by accepting the electron from the reduced metal complex as shown in the equation below[35,36]:

$$H^+ + RR'NO\bullet + Fe^{2+} \rightarrow RR'NOH + Fe^{3+}$$

Conclusions

The studied organic salts of imidazole derivatives salicylic aldehyde have appeared to be stronger antiproliferative agents against cancerous cells than the analogous spiropyrans with methyl imidazole derivative having higher activity than that of carboplatinum. At the same time, the toxicity of all studied compounds has appeared to be lower than that of carboplatin. Inhibition of ectonucleotidase has been detected as one of the certain mechanism of antiproliferative activity of the studied compounds. Moreover, no production of singlet oxygen has been detected after irradiation of compounds in TEMPOL assay, while the compounds have appeared to be moderate antioxidants in DPPH assay. To our best knowledge, this is the first study on OSILs antiproliferative activity with a multilateral exploration of its mechanisms.

Experimental Section

Chemistry

Synthesis of 5-chloromethylsalicylic aldehyde: salicylic aldehyde (10 g, 0.082 mol) has been added drop-wise at vigorous stirring paraformaldehyde (7.5 g) in HCl (150 mL, ~30 wt. %). The mixture has been stirred at room temperature for 24 h. The formed precipitate has been subjected to filtration and washed with diethyl ether. η = 55%. mp: 80°C.

Synthesis of 1-alkylimidazole derivatives of 5-chloromethylsalicylic aldehyde **1 - 4**: 5-chloromethylsalicylic aldehyde (0.009 mol) has been dissolved in acetonitrile (10 mL). To the formed solution, 3-alkylimidazole (0.009 mol) has been added. The mixture has been heated with reflux at stirring for 6 h. The reaction advance has been checked by TLC. The product has been filtrated, washed with hexane and ether, and dried. **1** (50.00%), mp: 86 - 90°C, IR (powder): 315, 3091, 2961, 1650, 1592, 1485, 1388, 1346, 1270, 1212, 1147, 1077, 1066, 1057, 973, 963, 948, 937 cm^{-1}.

2 (75.38%), mp: 70 - 73°C, IR (powder): 3142, 3119, 3085, 1846, 1651, 1555, 1484, 1390, 1352, 1324, 1271, 1202, 1147, 1077, 1007, 976, 944, 920 cm^{-1}.

3 (57.76%), mp: 113 - 115°C, IR (powder): 3147, 3094, 2980, 1722, 1651, 1567, 1484, 1390, 1349, 1324, 1275, 1199, 1146, 1087, 1025, 980, 960, 945 cm^{-1}.

4 (64.00%), mp: 134-136 °C, IR (powder): 3148, 3123, 3099, 1721, 1625, 1566, 1485, 1389, 1351, 1323, 1274, 1237, 1201, 1146, 1076, 1066, 1057, 982, 960, 944 cm^{-1}.

Crystal data for **4**: $C_{12}H_{13}Cl_4FeN_2O_2$, Mr = 414.89, monoclinic, space group $P2_1/n$ (no. 14), a = 6.7371(13) Å, b = 8.2079(16) Å, c = 30.517(6) Å, β = 94.07(3)°, V = 1683.3(6) $Å^3$, Z = 4, T = 298(2) K, D_c = 1.637 g cm^{-3}, F(000) = 836, R_1 = 0.0404 (191 parameters), wR_2 = 0.1015 [I ≥ 2σ(I)], GOF = 0.914 for all 13017 data. CCDC no. 1859770 (**4**). The structures were solved by direct methods and refined by full-matrix least-squares using the SHELXTL program suite.[36]

Synthesis of spiro compounds **5'-8'**: a 1-alkylimidazole derivative of 5-chloromethylsalicylic aldehyde (**1 – 4**, 0.0059 mol) has been dissolved in ethanol 95% (10 mL). 2 drops of catalyst triethylamine have been added, as well as 1,3,3-trimethyl-2-methyleneindoline (0.0063 mol) freshly distilled under vacuum. The mixture has been subjected to reflux for 8 h. The ethanol has been eliminated at the rotary evaporator. The left precipitate has been washed with hexane and diethyl ether.

Synthesis of tetrachloroferrate salts of spiro-compounds **5 – 8**: one of the spiro compounds **5'-8'** (0.002 mol) has been dissolved in methanol and $FeCl_3 \cdot 6H_2O$ (0.003 mol) has been added. The mixture has been refluxed for 5 hours, then the methanol has been eliminated at rotary evaporator and the left precipitate has been washed with diethyl ether.

6 (81.80%), mp: 165 - 170°C, IR (powder): 2987, 2902, 1590, 1533, 1476, 1451, 1404, 1309, 1260, 1153, 1114, 1076, 1066, 1057, 965, 933 cm^{-1}.

7 (70.71%), mp: 166 - 170°C, IR (powder): 2988, 2902, 1649, 1590, 1532, 1475, 1454, 1405, 1369, 1312, 1261, 1158, 1116, 1076, 1066, 1057, 967, 953, 923 cm^{-1}.

8 (84.55%), mp: 125 - 130°C, IR (powder): 2973, 2902, 1648, 1589, 1529, 1454, 1404, 1311, 1260, 1156, 1115, 1076, 1066, 1056, 966, 936 cm^{-1}.

Cell Transfection with e5'NT and preparation of membrane fractions

The COS-7 cells were transfected with a plasmid expressing e5'NT (human and rat)[37] in 10 cm plates by lipofectamine.[38] The confluent (80-90%) were further incubated for 5 h at 37 °C in simple DMEM (Dulbecco's modified Eagle's medium) containing plasmid DNA (6 µg) and lipofectamine reagent (24 µL). The reaction was terminated by diluting the reaction mixture with the same volume of DMEM/F-12 containing foetal bovine serum (20% FBS). Finally the cells were collected after 40-72 h. The collected cells were washed in triplicate with cool (4°C) tris-saline buffer and were separated from the harvesting buffer (0.1 mM phenylmethylsulfonyl fluoride (PMSF), 45 mM Tris buffer and 95 mM NaCl, pH 7.5) by scraping. This procedure was followed by the twice centrifugation of these cells at 300×g for 5 min. at 4°C[37]. These cells were again suspended in the harvesting buffer comprising aprotonin (10 µg/mL) and finally sonicated. Cellular and nuclear debris were removed from the media by centrifugation at 300×g at 4 °C for 10 min. For preservation glycerol (7.5%) was mixed with the resultant supernatant and stored at -80 °C for further use. Bradford microplate assay was employed for estimation of protein concentration using bovine serum albumin as a standard protein.[39]

Ecto-5'-Nucleotidase Inhibition Assay

The enzyme inhibition assay against human and rat e5'NTs was carried out according to the previously described method.[40] In this method, P/ACE MDQ capillary electrophoresis system (Beckman Instruments, Fullerton, CA, USA) was used that utilized a UV detection system for evaluation. The selected compounds were prepared in 10% DMSO as a stock solution with concentration 10 mM and further diluted in assay buffer (10 mM Tris HCl of pH 7.4 containing 1 mM $CaCl_2$ and 2 mM $MgCl_2$) to get working solutions (1 mM). The reaction was proceeded carrying 100 µL of total assay volume with 70 µL of assay buffer, 10 µL of test compound followed by the addition of 10 µL of *h*-e5'NT (6.94 ng) or *r*-e5'NT (7.17 ng) protein extracts. The mixture was incubated at 37 °C for 10 min and finally 10 µL of AMP substrate (0.5 mM) was added to start the reaction. The reaction mixture was allowed to incubate again at 37 °C for 20 min. At the end, the reaction vials were kept in a water bath (90 °C) for 20 min to denature protein and stop the reaction. Then 50 µL of each reaction mixture was transferred into a mini CE vial and hydro-dynamically (0.5 psi) injected into the capillary by taking 5s. The electro-osmatic separation of peaks i.e., substrate and product happened by applying a higher voltage (15 kV). The area under its absorbance peak was calculated for the estimation of product concentration i.e., adenosine at 260 nm. The compounds that exhibited ≥50 inhibition against either *h*-e5'NT or *r*-e5'NT enzyme were further investigated for their IC_{50} values. The experiment was carried out in triplicate by using the above mentioned experimental procedure.

Cell lines and cell cultures

HeLa cells, MCF-7 cells and BHK-21 cells were cultured in DMEM medium supplemented with penicillin (100 U/mL), streptomycin (100 µg/mL) and heat-inactivated FBS (10%). Similarly k-562 cells were cultured in RPMI-1640 medium containing the same additional composition as earlier. These cell lines were cultured and incubated in separate culture flasks at 37 ºC in 5% CO_2 incubator. The confluent monolayer cells (1×10^4 cells/mL) were seeded in 96-well plate to conduct initial cytotoxicity experiments.

Cell Viability Assays (MTT Assay)

The in-vitro MTT (dimethyl–2–thiazolyl–2,5–diphenyl–2*H*–tetrazolium bromide)–based cell viability assay was used for the determination of the cytotoxic potential of selected derivatives against breast cancer cells i.e., MCF-7 and cervical cancer cells i.e., HeLa. The assay was performed according to a previously described method of Mosmann[41] and Niks and Otto.[42] Total 90 µL of the cell culture containing 2.5×10^4 cells/ mL were seeded in 96–well flat–bottom plates. After that, test compound solution i.e. 10 µL (at a final concentration of 100 µM) was added to the respective wells and plates were kept for incubation at 37ºC for 24 h. A 100 µL of culture medium without any compound was taken as negative control. Carboplatin was taken as positive control. After incubation, MTT reagent (10 µL) was added to each well and again incubated for 4 h at 37ºC. Stopping reagent (100 µL, 50% isopropanol and 50 mL of 10% sodium dodecyl sulfate) was added to stop the enzyme reaction. The plates were incubated under agitation at room temperature for an additional 30 min. Finally change in absorbance was measured at 570 nm after subtracting the background signal (690 nm), using a 96–well microplate reader (Bio–Tek ELx 800TM, Instruments, Inc. Winooski, VT, USA). The activity of mitochondrial dehydrogenases of metabolically active cells resulted in the formation of formazan that represented the number of viable cells. All experiments were performed in triplicate and results were reported as percent inhibition values with a mean of three independent experiments (± SEM).

Cell Cycle Analysis Assay

The cell cycle analysis of the potent anticancer compounds was carried out as described previously.[43] The cells were incubated with different compounds for 24 h. Then the cells pellets were formed by centrifugation at 3000 rpm for 5 min. and cells were again allowed to resuspend in 3% FBS (200 µL). This step is followed by the addition of propidium iodide (5 µL, 250 µg/mL), Triton X-100 (5 µL, 10%) and ribonuclease A (25 µL, 10 mg/mL) in each vial and incubated in dark room for 1 h then these samples were evaluated by BD Accuri flow cytometer and 10,000 events were collected for each sample. The collected data were analyzed by using BD Accuri software. Carboplatin was considered as a positive control and the same procedure was repeated for carboplatin.

DNA Interaction Studies

The most potent compounds were further evaluated by performing their DNA interaction studies by using the previously reported method with slight modification.[44] The concentrations of DNA were determined at 260 nm by using micro-plate reader FLUOstar Omega. By using the molar absorption coefficient of 6600 $M^{-1}cm^{-1}$, the concentration of DNA was found as 4.15×10^{-4} M at 260 nm. Then different concentrations of DNA i.e. 0, 40, 90, 140, 190, 240, 290, and 340 µM were allowed to interact with fixed concentrations of compound **4** i.e., 40 µM and their reference solution. Then plates were allowed to incubate for 30 min. at room temperature. The absorption spectra were measured by using 96-well plates of 5.5 mm path length with blank correction. All the experiments were performed in triplicate. The mode of interaction of compounds was determined by using Omega–Data Analysis Software, Program Version: 3.00 R3. DNA interaction studies for carboplatin as a positive control was also performed.

Evaluation of Apoptosis by fluorescence microscopy

Morphological analysis of apoptosis was determined by using 4',6-diamidino-2-phenylindole (DAPI) and propidium iodide (PI) dyes. The specified amounts of cells (1.2×10^6) were cultured in 24-well plates along with coverslips overnight. Next day, 100 µM of the most potent compound i.e. **4** (IC_{50} =1.14 µM) was treated with the cells along with the negative and positive control i.e. carboplatin. The plate was allowed to incubate at 37ºC in CO_2 (5%) for 24 h. After incubation the cells were fixed and washed with Formalin (4%) and PBS (pH 7), respectively.

Finally, the cells were stained with DAPI or PI (10µg/ml) and incubated for 10 min in dark at room temperature and then examined under a fluorescence microscope (Nikon Eclipse-Ni Japan) at an excitation (358 nm) and emission (461 nm) wavelengths.[45]

Evaluation of antioxidant activity using a stable free radical diphenylpicrylhydrazyl(DPPH)

The method has been adapted according to the recommendations by Molyneux P (2004) as following: the calibration curve was built for DPPH, by preparing the free radical solutions of 10^{-5} – 10^{-4} M in methanol and measuring their absorbance at 516 nm. For the analyses, 10^{-4} M stock solutions of DPPH and of the studied compound were prepared. Then, six analytical solutions containing 1.5 mL DPPH stock solution and varying volumes of analytical solution of the compound from 0 to 1.5 mL along with the addition of methanol were prepared to reach the total volume of 3 mL solutions. At the moment of preparation of each analytic solution, the time was set for 30 min. After 30 min, the absorbance at 516 nm was read. For each solution, the percentage of the left DPPH is calculated taking into consideration the absorbance of the reference solution after 30 min, which is 100%. The molar ratio equals to the initial concentration of the compound solution divided by the initial concentration of the DPPH solution. Then, EC_{50} is determined which is equal to the molar ratio at the 50% of the DPPH left in solution. Reaction molecularity was determined as $\sigma = 1/(2 \cdot EC_{50})$.

Electron spin resonance investigation

The detection of the $^1O_2$ generated in solution in the presence of the photocatalysts was carried out through electron spin resonance (ESR) spectroscopy in order to confirm the activity of the photocatalysts. More details are provided in our previous publication.[36]

Acknowledgements

V.B. and F.M. are grateful for the funding support offered by the Science and Technology Center in Ukraine and the National Agency for Research and Development of the Republic of Moldova under international project 17.80013.8007.10/6245STCU. F.M. and D.P. are grateful for the funding offered by the BMBF project 01DK13029 and Prof. Dr. Annie K. Powell (Karlsruhe Institute of Technology, Germany) for generous support. V.B. and D.P. are grateful for the generous support from the Alexander von Humboldt Foundation. J.I. is grateful to the Higher Education Commission of Pakistan for the financial support through Project No. 20-3733/NRPU/R&D/ 14/520. The authors acknowledge the contributions and are grateful to Dr. A. Paul (ESR facilities) from the BAM Federal Institute for Materials Research and Testing, Berlin, Germany. The authors also gratefully acknowledge Prof. Dr. George E. Kostakis (University of Sussex, UK) for help with preliminary single crystal x-ray diffraction experiments.

Keywords: cancer • ionic liquids • organic salts • ectonucleotidase • antioxidant

References:

[1] K. R. Seddon, *J. Chem. Technol. Biotechnol.* **1997**, *68*, 351–356.

[2] T. Welton, **1999**, DOI 10.1021/CR980032T.

[3] P. Wasserscheid, W. Keim, *Angew. Chemie* **2000**, *39*, 3772–3789.

[4] N. V. Plechkova, K. R. Seddon, *Chem. Soc. Rev.* **2008**, *37*, 123–150.

[5] P. Nockemann, B. Thijs, S. Pittois, J. Thoen, C. Glorieux, K. Van Hecke, L. Van Meervelt, B. Kirchner, K. Binnemans, *J. Phys. Chem. B* **2006**, *110*, 20978–20992.

[6] A.-V. Mudring, *Aust. J. Chem.* **2010**, *63*, 544.

[7] D. Prodius, F. Macaev, E. Stingaci, V. Pogrebnoi, V. Mereacre, G. Novitchi, G. E. Kostakis, C. E. Anson, A. K. Powell, *Chem. Commun.* **2013**, *49*, 1915.

[8] D. Prodius, H. S. Shah, J. Iqbal, A. Macaeva, A. Dimoglo, G. E. Kostakis, N. Zill, F. Macaev, A. K. Powell, *Chem. Commun.* **2014**, *50*, 4888–4890.

[9] D. Prodius, V. Smetana, S. Steinberg, M. Wilk-Kozubek, Y. Mudryk, V. K. Pecharsky, A.-V. Mudring, *Mater. Horizons* **2017**, *4*, 217–221.

[10] A. Van den Bossche, E. De Witte, W. Dehaen, K. Binnemans, *Green Chem.* **2018**, *20*, 3327–3338.

[11] D. Prodius, M. Wilk-Kozubek, A.-V. Mudring, IUCr, *Acta Crystallogr. Sect. C Struct. Chem.* **2018**, *74*, 653–658.

[12] A. Balk, U. Holzgrabe, L. Meinel, *Eur. J. Pharm. Biopharm.* **2015**, *94*, 291–304.

[13] R. F. M. Frade, A. Matias, L. C. Branco, C. A. M. Afonso, C. M. M. Duarte, *Green Chem.* **2007**, *9*, 873–877.

[14] V. Kumar, S. V. Malhotra, *Bioorg. Med. Chem. Lett.* **2009**, *19*, 4643–4646.

[15] N. Kaushik, P. Attri, N. Kaushik, E. Choi, *Molecules* **2012**, *17*, 13727–13739.

[16] C. Suresh, H. Zhao, A. Gumbs, C. S. Chetty, H. S. Bose, *Bioorg. Med. Chem. Lett.* **2012**, *22*, 1734–1738.

[17] R. Ferraz, J. Costa-Rodrigues, M. H. Fernandes, M. M. Santos, I. M. Marrucho, L. P. N. Rebelo, C. Prudêncio, J. P. Noronha, Ž. Petrovski, L. C. Branco, *ChemMedChem* **2015**, *10*, 1480–1483.

[18] R. F. M. Frade, A. A. Rosatella, C. S. Marques, L. C. Branco, P. S. Kulkarni, N. M. M. Mateus, C. A. M. Afonso, C. M. M. Duarte, *Green Chem.* **2009**, *11*, 1660–1665.

[19] S. V. Malhotra, V. Kumar, *Bioorg. Med. Chem. Lett.* **2010**, *20*, 581–585.

[20] X. Wang, C. A. Ohlin, Q. Lu, Z. Fei, J. Hu, P. J. Dyson, *Green Chem.* **2007**, *9*, 1191–1197.

[21] S. Marquis, B. Ferrer, M. Alvaro, H. García, D. R. Heinz, *J. Phys. Chem. B* **2006**, *110*, 14956–14960.

[22] K. S. Egorova, E. G. Gordeev, V. P. Ananikov, *Chem. Rev.* **2017**, *117*, 7132–7189.

[23] A. R. Dias, J. Costa-Rodrigues, M. H. Fernandes, R. Ferraz, C. Prudêncio, *ChemMedChem* **2017**, *12*, 11–18.

[24] R. H. Liu, *J. Nutr.* **2004**, *134*, 3479S–3485S.

[25] K. Scheit, G. Bauer, *Carcinogenesis* **2015**, *36*, 400–411.

[26] M. Riethmüller, N. Burger, G. Bauer, *Redox Biol.* **2015**, *6*, 157–168.

[27] M. Cai, Y. Liang, M. Yao, Y. Xia, F. Zhou, W. Liu, *ACS Appl. Mater. Interfaces* **2010**, *2*, 870–876.

[28] M. Cai, Y. Liang, F. Zhou, W. Liu, *J. Mater. Chem.* **2011**, *21*, 13399.

[29] Y. Lion, M. Delmelle, A. Van de Vorst, *Nature* **1976**, *263*, 442–443.

[30] Y. Nosaka, H. Natsui, M. Sasagawa, N. Atsuko Y., *J. Phys. Chem. B* **2006**, *110*, 12993–12999.
[31] X. Guo, D. Zhang, G. Zhang, D. Zhu, *J. Phys. Chem. B* **2004**, *108*, 11942–11945.
[32] S. Kume, H. Nishihara, *Dalt. Trans.* **2008**, *0*, 3260–3271.
[33] S. Nagashima, M. Murata, H. Nishihara, *Angew. Chemie Int. Ed.* **2006**, *45*, 4298–4301.
[34] S. V. Paramonov, V. Lokshin, O. A. Fedorova, *J. Photochem. Photobiol. C Photochem. Rev.* **2011**, *12*, 209–236.
[35] J. B. Mitchell, A. Samuni, M. C. Krishna, W. G. DeGraff, M. S. Ahn, U. Samuni, A. Russo, *Biochemistry* **1990**, *29*, 2802–2807.
[36] M. Neamțu, F. Macaev, V. Boldescu, V.-D. Hodoroaba, C. Nădejde, R. J. Schneider, A. Paul, G. Ababei, U. Panne, *Appl. Catal. B Environ.* **2016**, *183*, 335–342.
[37] Y. Bravo, P. Teriete, R. P. Dhanya, R. Dahl, P. S. Lee, T. Kiffer-Moreira, S. R. Ganji, E. Sergienko, L. H. Smith, C. Farquharson, et al., *Bioorganic Med. Chem. Lett.* **2014**, *24*, 4308–4311.
[38] F. Kukulski, S. A. Lévesque, É. G. Lavoie, J. Lecka, F. Bigonnesse, A. F. Knowles, S. C. Robson, T. L. Kirley, J. Sévigny, *Purinergic Signal.* **2005**, *1*, 193–204.
[39] M. M. Bradford, *Anal. Biochem.* **1976**, *72*, 248–254.
[40] P. A. Channar, S. J. A. Shah, S. Hassan, Z. un Nisa, J. Lecka, J. Sévigny, J. Bajorath, A. Saeed, J. Iqbal, *Chem. Biol. Drug Des.* **2017**, *89*, 365–370.
[41] T. Mosmann, *J. Immunol. Methods* **1983**, *65*, 55–63.
[42] M. Nikš, M. Otto, *J. Immunol. Methods* **1990**, *130*, 149–151.
[43] Y. Saito, N. Uchida, S. Tanaka, N. Suzuki, M. Tomizawa-Murasawa, A. Sone, Y. Najima, S. Takagi, Y. Aoki, A. Wake, et al., *Nat. Biotechnol.* **2010**, *28*, 275–280.
[44] M. Sirajuddin, S. Ali, V. McKee, S. Zaib, J. Iqbal, *RSC Adv.* **2014**, *4*, 57505–57521.
[45] R. Vidya Priyadarsini, R. Senthil Murugan, S. Maitreyi, K. Ramalingam, D. Karunagaran, S. Nagini, *Eur. J. Pharmacol.* **2010**, *649*, 84–91.

Entry for the Table of Contents

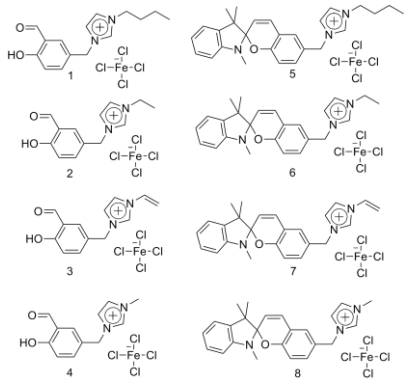

The reported tetrachloroferrate salt of 1-methylimidazole derivative of salicylic aldehyde has higher cytotoxicity towards HeLa cells and lower cytotoxicity towards BHK-21 cells as compared to carboplatinum. The compound induces stronger inhibition of ectonucleotidase than carboplatinum, the effect being one of the main mechanisms of its antiproliferative activity.